

# Enhanced Removal of Ni<sup>2+</sup> and Cu<sup>2+</sup> Using Biochar/Polyaniline Composites: A Comparative Study of In-Situ and Ex-Situ Polymerization Methods

Ravi Varma Sudaya<sup>1</sup>, Min Rui Chia<sup>2</sup>, Peratiikka Selvum<sup>1</sup>, Sook-Wai Phang<sup>1</sup> and Kian Wei Chong<sup>1\*</sup>

<sup>1</sup>Department of Physical Science, Faculty of Applied Sciences, Tunku Abdul Rahman University of Management and Technology (TAR UMT), Jalan Genting Klang, Setapak, 53300 Kuala Lumpur, Malaysia

<sup>2</sup>Department of Chemical Sciences, Faculty of Science and Technology, Universiti Kebangsaan Malaysia, 43600 Bangi, Selangor, Malaysia

\*Corresponding author (e-mail: chongkw@tarc.edu.my)

Industrial revolution and population growth result in heavy metal pollution. There is various research done on heavy metal removal, nonetheless most of the conventional methods are associated with high costs and poor performance. This study investigates the development of polyaniline-supported biochar (BC/PANI) composites as efficient adsorbents for removing heavy metal ions (Ni<sup>2+</sup> and Cu<sup>2+</sup>) from aqueous solutions. These BC/PANI composites were examined as a promising material in removing heavy metal ions, specifically Ni<sup>2+</sup> and Cu<sup>2+</sup>, from aqueous environments. Fourier-transform infrared spectrometry (FT-IR) analysis revealed the presence of hydroxyl, carbonyl, alkane, and alkene groups in BC, while amine, aromatic, and alkane groups were found on PANI and the composites. Ultraviolet-visible (UV-Vis) analysis confirmed the conductive emeraldine salt state of PANI and scanning electron microscope (SEM) images showed that the composites had pore sizes similar to pure BC, which could enhance their thermal stability. The electrical conductivity of the composites ( $8.0 \times 10^{-1} - 5.6 \text{ Scm}^{-1}$ ) was slightly lower than that of pure PANI ( $6.0 - 8.0 \text{ Scm}^{-1}$ ). Preliminary results indicated that the BC/PANI (ex-situ) composite achieved Ni<sup>2+</sup> and Cu<sup>2+</sup> removal efficiencies of 79.61% and 68.87%, respectively, while optimal conditions for Ni<sup>2+</sup> removal (81.56%) were found at pH 5, 30 minutes contact time and by using 0.75 g of adsorbent. In-situ polymerization achieved superior removal efficiency (83% for Ni<sup>2+</sup>) with minimal adsorbent use compared to the ex-situ method (69.4%), showcasing its potential for efficient metal ion removal. These findings highlight the potential of BC/PANI composites as sustainable and cost-effective solutions for water purification and heavy metal remediation, realizing the Sustainable Development Goal 6: Clean Water and Sanitation.

**Keywords:** Biochar; polyaniline; composites; adsorption; heavy metal removal

*Received: December 2024; Accepted: February 2025*

Heavy metal pollution is a significant environmental concern in Malaysia, primarily due to the rapid industrial, population, and economic growth, leading to increased waste, where heavy metals tend to accumulate in the food chain and pose serious health risks due to their resistance against metabolization [1, 2]. Although various heavy metal removal methods have been studied by researchers, traditional removal methods, such as membrane filtration and chemical precipitation, often face limitations like low efficiency and high costs, prompting the exploration of adsorption techniques [3]. On the other hand, adsorption method is relatively more feasible due to the simplicity, low costs, high efficiency, and most importantly, more environmentally friendly [4]. This underscores the need for innovative and sustainable solutions like biochar-supported polyaniline (PANI/BC) composites.

Biochar (BC) stands out due to its high surface area, unique porous structures, and stable chemical properties, which enhance its capacity for heavy metal adsorption, including but not limited to copper (Cu), zinc (Zn), nickel (Ni), and mercury (Hg) [4]. In addition, there are abundant sources of BC materials such as leaves, sludge, and crop stalks. In Malaysia, the palm oil industry generates substantial amounts of empty fruit bunch (EFB) waste, which can lead to environmental contamination if improperly processed [5]. Converting EFB into BC through pyrolysis yields a stable product beneficial for soil health and carbon sequestration [6]. Nonetheless, the heavy metal adsorption performance of BC is often affected by the raw materials, type of heavy metals, adsorption condition, and ageing when exposed to the environment. These factors may limit the robustness of pure BC as the adsorbent for heavy metal removal. Therefore, the

modification of the chemical features of BC is often studied to improve its adsorption flexibility.

Polyaniline (PANI), a conducting polymer, is also an effective adsorbent of heavy metals due to its stability, affordable price, easy synthesis, and high conductivity [7]. PANI possesses  $\pi$ -conjugated system, hole conducting structures, and electron-donating amine derivatives which could enhance its chemical interactions with heavy metals, rendering it the excellent chelating capabilities [8]. Although PANI has minimal toxicity, integrating BC with PANI can improve the composite's mechanical strength and stability, thereby enhancing heavy metal removal without affecting the performance of BC [9].

However, studies on their combined effects for heavy metal remediation remain limited. Previous research has primarily focused on ex-situ polymerization of PANI with bio-adsorbents, which may result in weaker bonds and reduced adsorption efficiency [10]. In contrast, in-situ polymerization may allow stronger interactions between BC and PANI, potentially enhancing adsorption efficiency [11]. This study aimed to synthesize and characterize PANI/BC composites using ex- situ and in-situ polymerization methods and evaluate their efficiency in removing Cu and Ni under varying conditions. As the result of the optimized heavy metal removal performance of PANI/BC composite, it has high potential to be applied in remediating rivers in Malaysia, such as Lohan River, and the Sungai Petani area that are heavily polluted by metals such as copper and nickel [12,13].

## MATERIALS AND EXPERIMENTAL

### Materials

Aniline monomer (ANI) ( $\geq 99.5\%$ ) and ammonium persulfate (APS) ((NH<sub>4</sub>)<sub>2</sub>S<sub>2</sub>O<sub>8</sub>) ( $\geq 98.0\%$ ) were purchased from Sigma-Aldrich (Burlington, USA). Acetone (CH<sub>3</sub>COCH<sub>3</sub>) ( $\geq 99.5\%$ ) from Bendosen Laboratory Chemicals (Istanbul, Turkey) was used in the washing process during the polymerization of PANI. Methanol (CH<sub>3</sub>OH) with a purity of ( $\geq 99.8\%$ ) was used to wash the polymer and was purchased from Sigma Aldrich. Distilled water was used as a solvent in the UV-Vis analysis of the characteristics of PANI. For the calcination of BC, oil palm EFB was obtained from Biovision Greenery SDN BHD in Segamat, Johor. During the application of heavy metal removal, nickel(II) sulfate hexahydrate (NiSO<sub>4</sub>·6H<sub>2</sub>O) and copper(II) sulfate pentahydrate (CuSO<sub>4</sub>·5H<sub>2</sub>O) were used throughout the synthesis and analysis, which were purchased from Sigma-Aldrich.

### Synthesis of Adsorbents

#### *Synthesis of BC*

EFB used in this project was factory-sourced. All the EFB was pyrolyzed using a tube furnace at a temperature of 600°C with a dwell time of 30 minutes under a nitrogen gas flow condition. The flow rate of nitrogen gas was kept at minimum, which was 1 L/min. The produced BC was ground well into a fine powder.

#### *Synthesis of PANI*

PANI was synthesized using a chemical oxidation process at 0°C, employing ammonium persulfate (APS) as the oxidizing agent and hydrochloric acid (HCl) as the dopant. A 0.2 M ANI/HCl solution was prepared by dispersing 1.82 mL of aniline monomer in 1 M HCl, while 5.71 g of APS was dissolved in distilled water to create a 0.25 M solution. Both solutions were stirred at 0°C, with APS being added gradually using a dropping funnel. Polymerization occurred overnight at this temperature with continuous stirring. The next day, the sample was washed three times with 1 M HCl and acetone to remove unreacted monomers, dopants, and contaminants. The green PANI precipitate was then dried in an oven at 60°C for 24 hours, ground into a fine powder, and further dried in a desiccator to minimize moisture.

#### *Synthesis of BC/PANI with different PANI% (ex-situ polymerization)*

For the first part of polymerization, BC/PANI composites were synthesized through ex-situ polymerization by fixing the amount of BC and varying the ratio of BC to PANI (1:0, 0:1, 1:0.01, 1:0.03, 1:0.05, 1:0.07, 1:0.1, 1:0.5, and 1:1). The weights of BC and PANI were blended with a mortar and pestle for approximately 3 minutes to obtain the BC/PANI composites.

#### *Synthesis of PANI/BC with different BC% (ex-situ and in-situ Polymerization)*

For the second part of polymerization, PANI/BC composites were synthesized through both ex-situ and in-situ polymerization by fixing the amount of PANI and varying the ratio of PANI to BC (1.85:0.03, 1.85:0.85, 1.85:0.27 and 1.85:0.37). For ex-situ polymerization, a similar procedure as BC/PANI (E) was carried out to produce PANI/BC (E). For in-situ polymerization, BC was dispersed in the dopant, HCl and shaken for 30 minutes using an orbital shaker before adding the aniline monomer. 0.25 M APS was gradually added to the 0.25 M ANI/HCl solution mixture slowly using a dropping funnel, while stirring

continuously. Polymerization was then conducted at 0°C overnight with constant stirring. The following day, similar filtration and washing procedures as synthesis of PANI were repeated to produce PANI/BC (I).

### Characterization of Adsorbents

#### *Characterization of BC and PANI*

BC and PANI were characterized using Fourier-Transform Infrared Spectroscopy (FTIR), Ultraviolet-Visible Spectrophotometry (UV-Vis), Scanning Electron Microscopy (SEM), and Thermogravimetric Analysis (TGA) to assess their chemical structure, oxidation state, surface morphology, and thermal stability. FTIR analyzed functional groups within the wavenumber range of 650–4000 cm<sup>-1</sup> using the Perkin Elmer Spectrum 100 ATR-FTIR spectrophotometer (Waltham, USA). FTIR analysis helps confirm the key functional groups in adsorbents, thus determining the oxidation states of PANI and chemical bonding of the composites. UV-vis spectra were recorded in the range of 200–900 nm with the Hitachi spectrophotometer UH5300 (Tokyo, Japan), to further reaffirm PANI's conducting states. SEM (Nanoeye SNE-3000M; Tokyo, Japan) was used to examine surface morphology and porosity of the BC composites, while TGA (TGA Q50 model; New Castle, USA) was conducted in the range of 30–900°C at a heating rate of 20°C/min to evaluate the composites' thermal stability. Additionally, the electrical conductivity of the PANI pellet was measured using a resistivity meter (Mitsubishi Chemical Analytech Model Loresta-GX; Yokohama, Japan) with a PSP probe. The PANI pellet was compressed into a 13 mm diameter pellet using a digital hydraulic press (PIKE Technologies Crush IR; Madison, USA), and its thickness was measured with a Mitutoyo digital micrometer (Kawasaki, Japan).

#### *Characterization of BC/PANI (E), PANI/BC (E) and PANI/BC (I)*

BC/PANI (E), PANI/BC (E), and PANI/BC (I) were characterized by FTIR, UV-VIS, SEM, TGA analyses, and electrical conductivity measurement to provide the information about chemical structure, oxidation state, surface morphology, conductivity, and thermal stability of the composites. Similar procedures had been carried out for pure BC and PANI.

### Application of BC/PANI (E) Composite in Heavy Metal Removal

Heavy metals such as nickel (Ni<sup>2+</sup>) and copper (Cu<sup>2+</sup>) were used to assess the removal efficiency (%) by BC/PANI (E), PANI/BC (E), and PANI/BC

(I) composites. The heavy metal removal efficiency of the composites is calculated using Equation 1:

$$\text{Removal Efficiency (\%)} = 100 \times \frac{(C_i - C_f)}{C_i} \quad \text{Equation 1}$$

Where, C<sub>i</sub> (ppm) = initial concentration of heavy metal solution and C<sub>f</sub> (ppm) = final concentration of heavy metal solution.

The removal efficiency of heavy metals (Ni<sup>2+</sup> and Cu<sup>2+</sup>) using BC/PANI (E) was evaluated by preparing salt solutions with an initial concentration of 100 ppm from nickel(II) sulfate and copper(II) sulfate, then diluting to standard concentrations of 2, 4, 6, 8, and 10 ppm. Concentration was measured using the Thermofisher ICE 300 Series AA model flame atomic absorption spectrometer (FAAS). 1 g of the BC/PANI (E) composite was mixed with 45 mL of Ni<sup>2+</sup> or Cu<sup>2+</sup> solution, shaken for 30 minutes, filtered through a 0.22 μm nylon filter, and repeated for another two times to obtain a triplicate set of data. A calibration curve for the metals was established using FAAS, and removal efficiencies were calculated to identify the metal with the highest removal efficiency for further optimization. ANOVA statistical analysis was performed.

### Optimization of Parameters to Increase Removal Efficiency of Heavy Metals By BC/PANI (E)

The study further analyzed the optimum Ni<sup>2+</sup> removal efficiency of the BC/PANI (E) composite by testing different weights (0.25 g, 0.50 g, and 0.75 g) of the composite under initial conditions. The highest removal efficiency at varying weights guided the subsequent analysis. Additionally, the experiment assessed different contact times (15, 30, 60, and 100 minutes) to determine their impact on removal efficiency. Lastly, various pH levels (2, 5, 7, 8, and 10) were also tested to evaluate their effects on heavy metal removal. All the experiments were repeated thrice.

### Application of PANI/BC (E) And PANI/BC (I) Composites in Heavy Metal Removal

After determining the optimum composite weight, contact time, and pH for heavy metal removal procedure, a similar procedure as the application of the BC/PANI (E) composite in heavy metals removal was carried out with 25 mL of 50 ppm of Ni<sup>2+</sup> solution and 0.1 g of PANI/BC (E) and PANI/BC (I) using the optimized parameters. The removal efficiency of the Ni<sup>2+</sup> solution was calculated by using Equation 1. Then, the removal efficiencies of Ni<sup>2+</sup> of PANI/BC (E) and PANI/BC (I) were compared. The complete methodology is summarized in Figure 1.

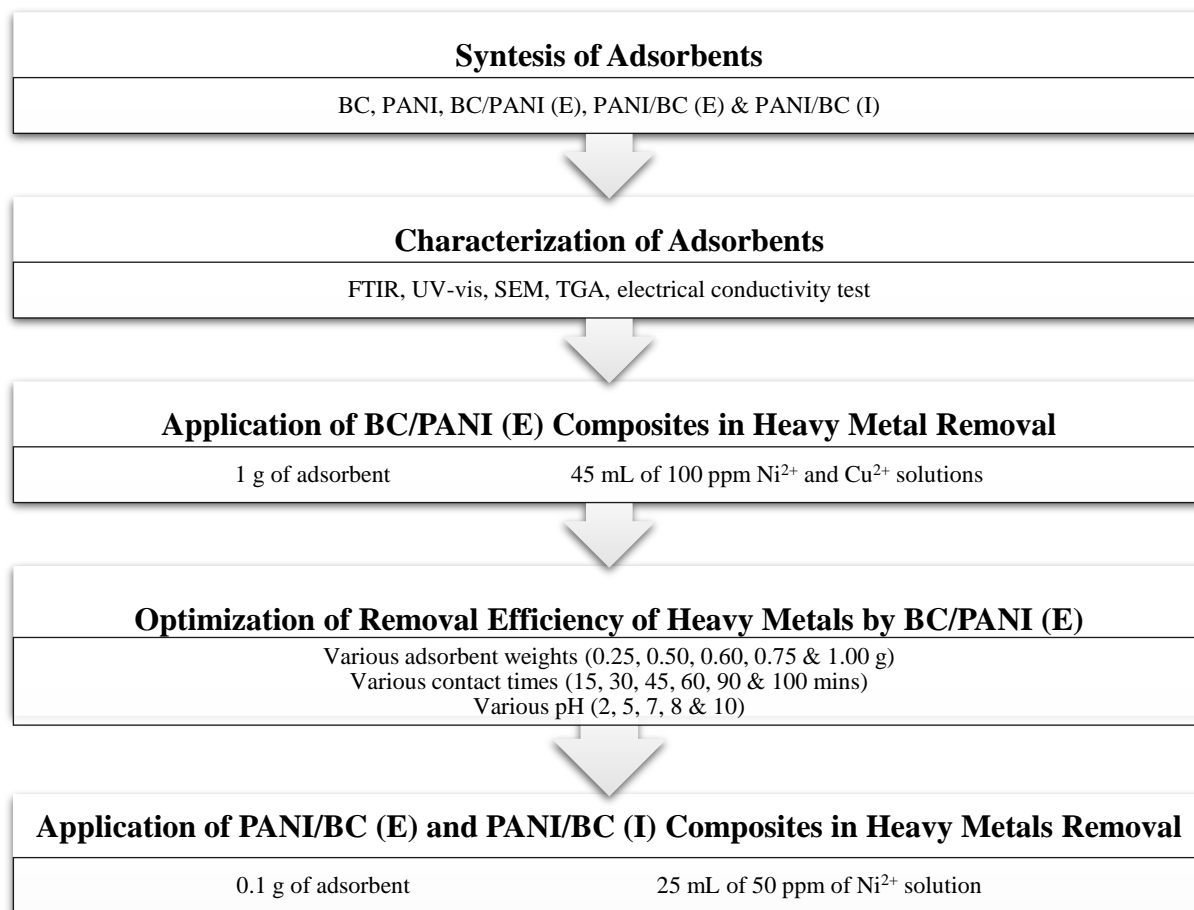


**Figure 1.** Flow diagram of the complete methodology.

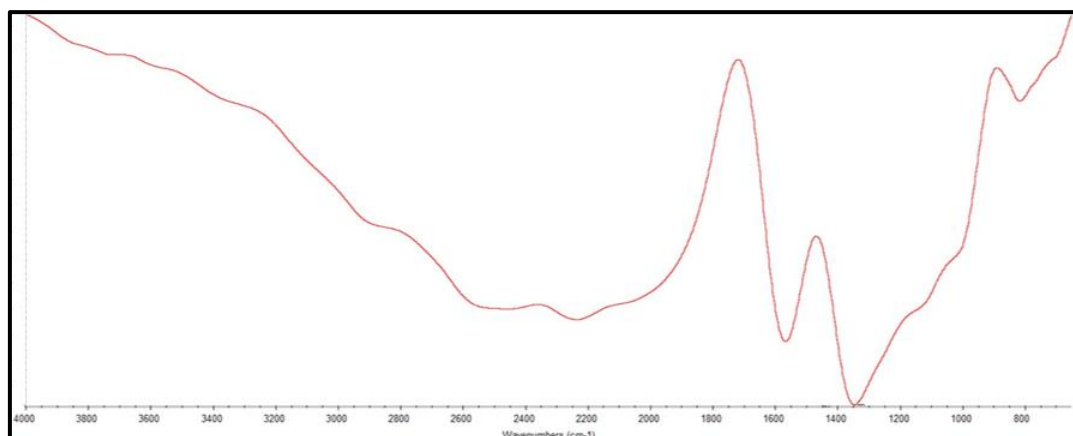
## RESULTS AND DISCUSSION

### Characterization

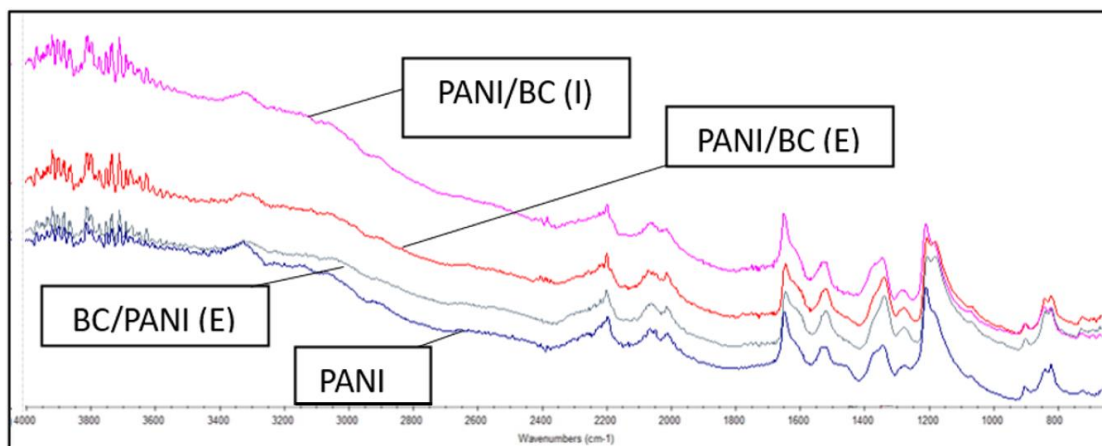
#### *Fourier-Transform Infrared Spectrometer (FTIR) Analysis*

Figure 2a displays the FTIR spectra of pure BC and PANI within the 650–4000 cm<sup>-1</sup> range. The BC spectrum features a broad peak at 3200–3400 cm<sup>-1</sup> indicative of O-H stretching from hydroxyl groups [14], along with bands at 800–900 cm<sup>-1</sup> for C-H bending and 1500–1600 cm<sup>-1</sup> for C=C stretching in aromatic and alkene compounds [15]. The intensity of the peaks is weak at high pyrolysis temperatures like 600°C. In contrast, PANI exhibits

a broad peak at 3200–3450 cm<sup>-1</sup> associated with N-H stretching due to protonation of nitrogen, peaks at 1550–1650 cm<sup>-1</sup> and 1350–1450 cm<sup>-1</sup> for C=C stretching from quinoid and benzenoid rings, respectively, and a band at 1270–1280 cm<sup>-1</sup> confirming C-N stretching, which indicates the conductive emeraldine salt form [16]. Figure 2b shows the FTIR spectra for the BC/PANI (E), PANI/BC (E), and PANI/BC (I) composites, all exhibiting similar peaks to PANI with no new peaks, suggesting that BC incorporation does not significantly alter PANI's chemical structure. The intensity of the peaks shows slight variations with different percentage of BC in the respective composites, becoming either broader or narrower, indicating interactions between BC and PANI [10].



(a)



(b)

**Figure 2.** FTIR spectra of (a) BC and (b) PANI, BC/PANI (E), PANI/BC (E) and PANI/BC (I).

#### UV-Vis Analysis

Figure 3a presents the UV-Vis spectra of pure BC and PANI, revealing no absorption peaks for BC, indicating its purity [17]. In contrast, PANI shows two peaks: one at 380–390 nm related to  $\pi \rightarrow \pi^*$  transitions, and another at 480–490 nm corresponding to polaron  $\rightarrow \pi^*$  transitions, confirming its doped and conducting state [18]. BC is known to have excellent UV shielding properties, thus BC has relatively higher absorbance [19]. Figure 3b shows the UV-Vis spectra of the BC/PANI

(E) (1:1), PANI/BC (E) (1:0.2), and PANI/BC (I) (1:0.2) composites, all exhibiting peaks at 380 nm and 482.5 nm, consistent with PANI's transitions. A broad band at 350–420 nm in the BC/PANI spectrum further supports the integration of BC with PANI, confirming that all composites contain PANI in the emeraldine salt state [20]. BC/PANI has a higher absorbance than PANI/BC (E) due to the higher BC composition. On the other hand, the reduction of absorbance in PANI/BC (I) shows that effective interaction between PANI and BC is established.

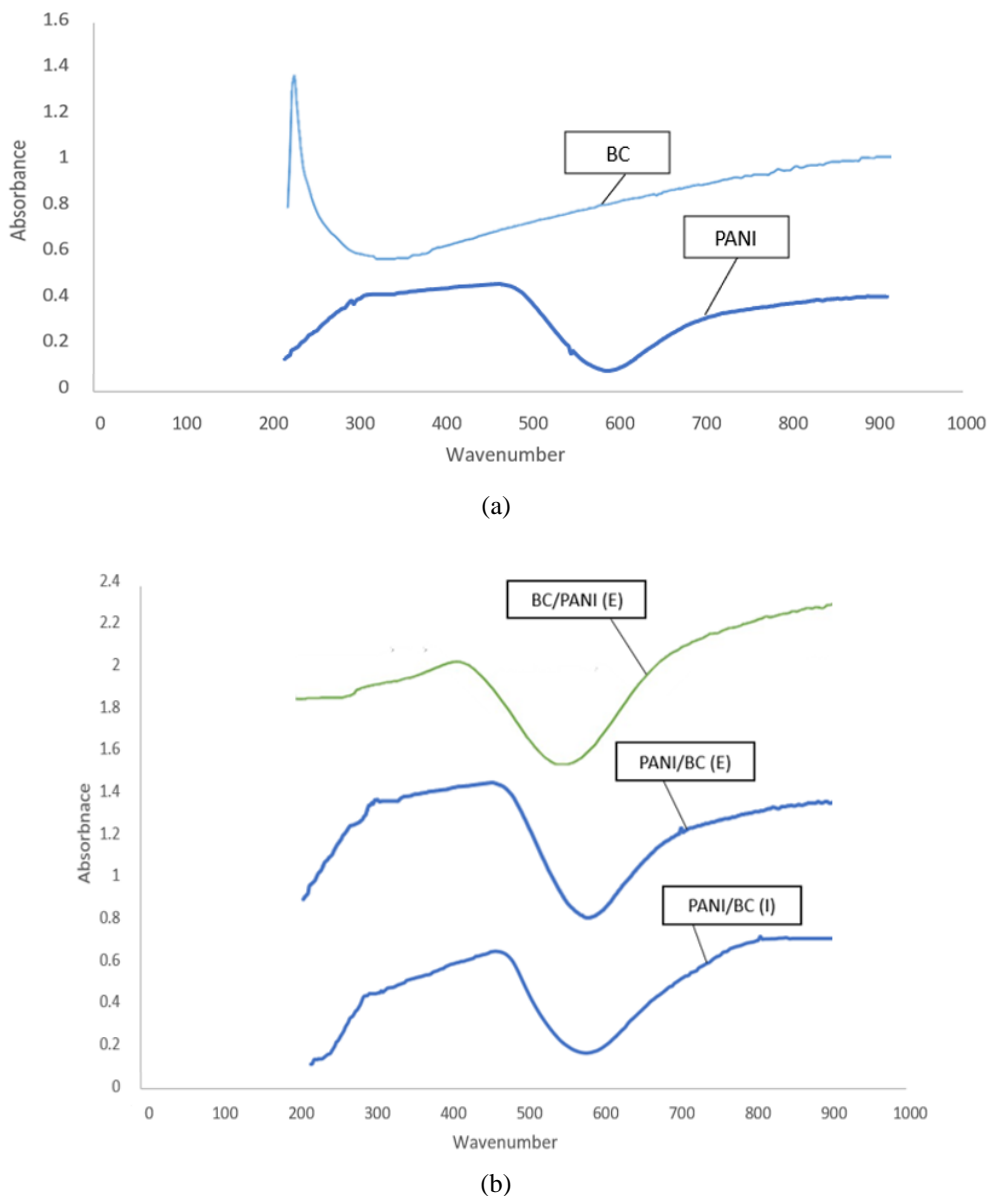


**Figure 3.** UV-Vis spectra of (a) pure BC and pure PANI and (b) BC/PANI (E), PANI/BC (E), and PANI/BC (I).

*Thermogravimetric Analysis*

Figure 4a displays the thermograms of BC, PANI, and the BC/PANI (E) (1:1) composite, while Figures 4b and 4c present the thermograms for PANI/BC (E) (1:0.2) and PANI/BC (I) (1:0.2), plotted as weight loss (%) against temperature (°C). BC experienced multiple thermal breakdown processes, with an initial moisture loss up to 150°C, followed by stability until 400°C, and significant weight loss between 360 and 800°C, yielding a 9.8% residue due to the breakdown of residual organic matter like cellulose and hemicellulose [17]. For PANI and its composites, three major weight loss stages were observed. The first stage (100-200°C) involved the loss of water and dopant HCl, the second stage (200-400°C) was attributed to the discharge of

protonic acid groups, and the highest weight loss occurred between 400-700°C due to thermal degradation of PANI [21]. At 900°C, the residues were 9.8% for BC, 28.94% for PANI, 31.55% for BC/PANI (E), 45.45% for PANI/BC (E), and 48.79% for PANI/BC (I), where the higher residual content of PANI/BC composites was due to the presence of the higher composition of PANI. The improved thermal stability of the BC/PANI composite is attributed to the presence of BC, which enhances PANI's thermal stability. The enhanced thermal stability demonstrates a strong prospect of adsorbent composites to be thermally regenerated for the restoration of adsorption capacity [22]. This reduces the PANI/BC composites' susceptibility against the change surface chemistry and porosity during the regeneration process.

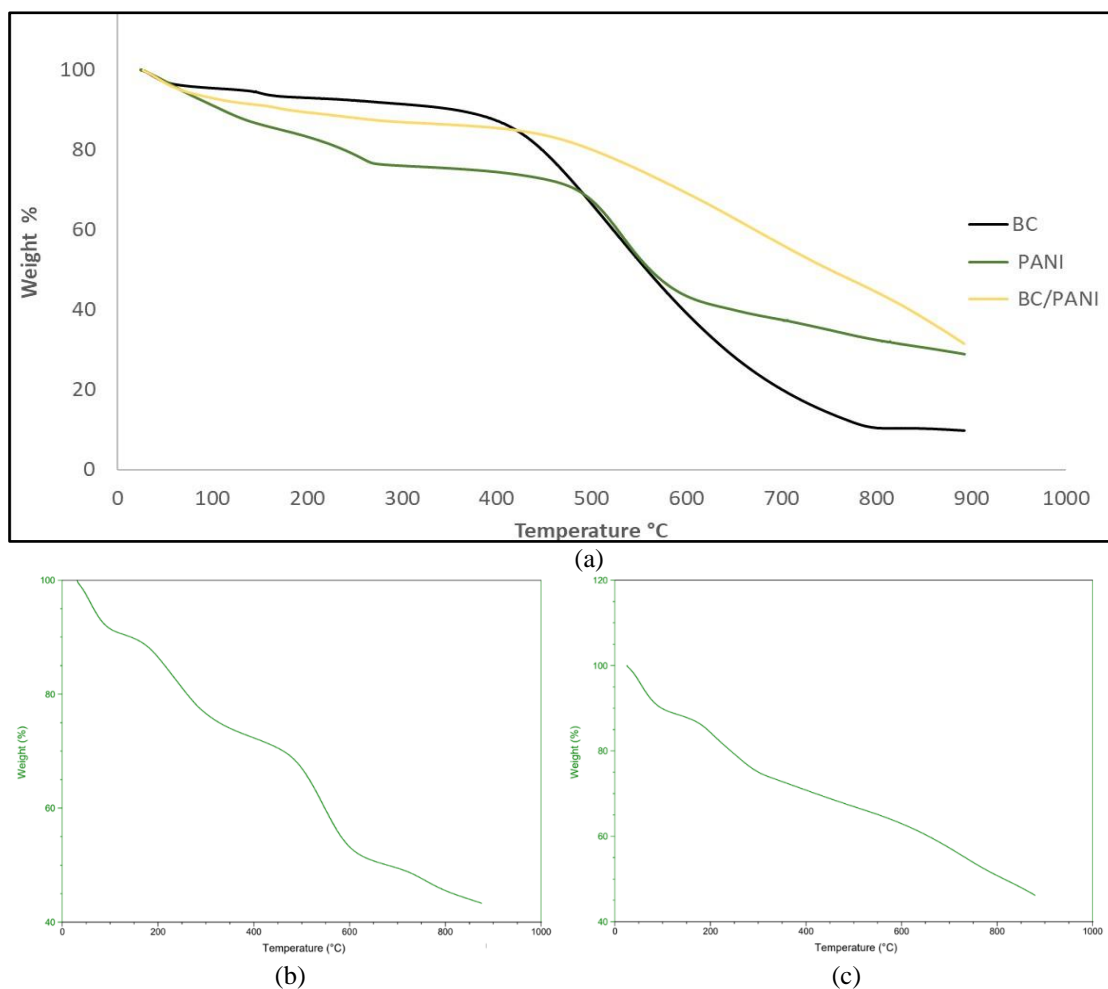


**Figure 4.** TGA of (a) BC, PANI and BC/PANI (E), (b) PANI/BC (E), and (c) PANI/BC (I).

### SEM Analysis

Figure 5a presents an SEM image of BC, highlighting its well-defined pores with sizes ranging from 10–20  $\mu\text{m}$  and a homogeneous arrangement. The analysis indicates that higher pyrolysis temperatures, like 600°C, enhance pore development and lead to more ordered aromatic structures and increased crystallinity due to organic material volatilization [23]. The porous structure of BC is essential for better polymer chains penetration which results in improved mechanical interlocking and a stronger BC–PANI interface [14]. Figure 5b displays PANI with rod-like aggregates and a honeycombed structure formed by linked fibrils, resulting from strong interactions in acidic environments [24].

Figure 5c shows the BC/PANI (E) composite, the integration of PANI onto the BC surface is clearly visible in SEM images where BC is uniformly coated

with PANI without altering the pore size. Figures 5d and 5e depict the SEM images of PANI/BC (E) and PANI/BC (I), respectively, revealing similar structures in both composites, characterized by tangled, tubular fibrous arrangements. Curved rod-shaped PANI aggregates are observed covering the porous surface of BC [25]. Specifically, larger PANI aggregates are observed in PANI/BC (E) when compared to PANI/BC (I) with a more uniform PANI interaction with BC. The larger PANI aggregates may lead to the heterogeneity of the composites, thus reducing the mechanical properties of the composites. On the other hand, PANI/BC (I) having relatively more compact structures and homogenous interactions of PANI with the BC fibers would exhibit improved electrical conductivity and mechanical strength, respectively [26]. Therefore, PANI/BC synthesized through the in-situ method can enhance both the electrical conductivity and mechanical performance of the composite through a stronger conducting fiber network.

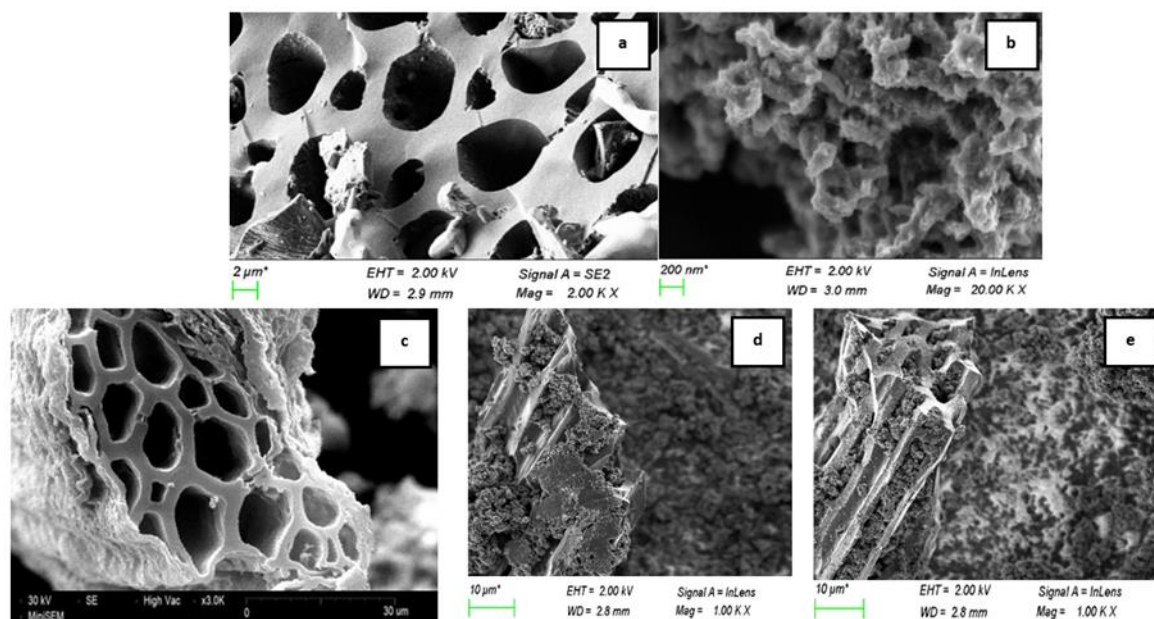


**Figure 5.** SEM images of (a) BC at 2000x magnification, (b) PANI at 20000x magnification, (c) BC/PANI (E) at 3000x magnification, (d) PANI/BC (E) at 1000x magnification, and (e) PANI/BC (I) at 1000x magnification.

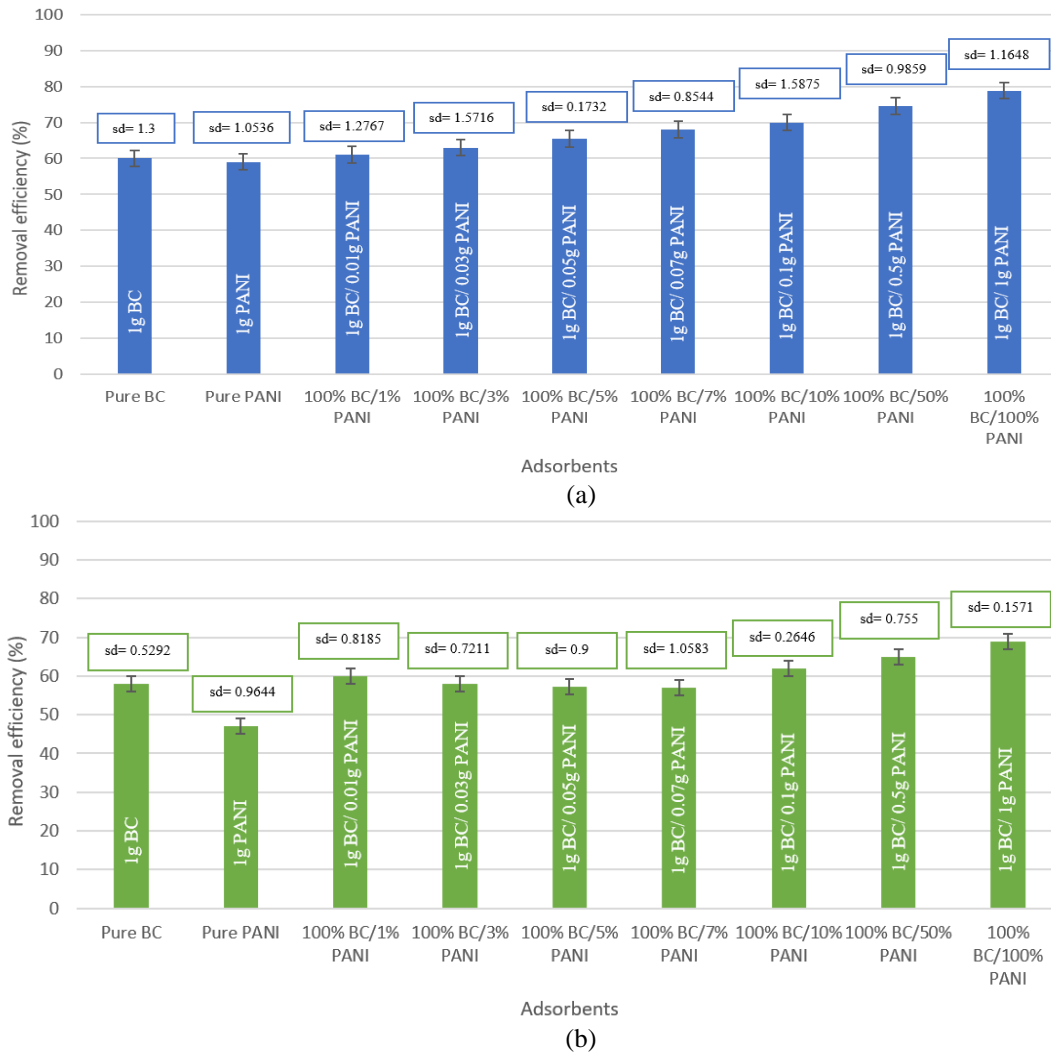
### Application of BC/PANI (E) Composite in Heavy Metal Removal

Figure 6a shows the Ni<sup>2+</sup> removal efficiency of pure BC, pure PANI, and BC/PANI (E) with varying percentages of PANI. The BC/PANI (E) composite exhibits a significant increase in removal efficiency compared to BC and PANI alone, achieving a maximum of 79.51% for Ni<sup>2+</sup> removal, whereas BC and PANI individually reach only 60–65%. The enhanced removal efficiency of BC/PANI is attributed to its high binding capacity for Ni<sup>2+</sup> and the functional groups activated on the adsorbents during the removal process. While BC has limited active sites (-OH and =O), the combination with PANI introduces additional functional groups (-H, =O, -NH, =N, and N<sub>2</sub>) [27]. The interaction of Ni<sup>2+</sup> with hydroxyl and amine groups in the BC/PANI (E) composite further facilitates removal of Ni<sup>2+</sup> [28]. Additionally, the increased surface area of the composite due to presence of BC in the composite contributes to a higher number of binding sites, thereby enhancing its overall removal efficiency of Ni<sup>2+</sup> [29].

Figure 6b shows the Cu<sup>2+</sup> removal efficiency of pure BC, pure PANI, and BC/PANI (E). Pure BC and pure PANI achieve Cu<sup>2+</sup> removal efficiencies of 59.4% and 47%, respectively. The lower adsorption rate for Cu<sup>2+</sup>, compared to Ni<sup>2+</sup>, is likely due to cationic repulsion between Cu<sup>2+</sup> and the protonated segments of PANI [30]. The BC/PANI (E) composite improves Cu<sup>2+</sup> removal efficiency to 68.87%,

attributed to the enhanced interaction from increased amine functional groups in the composite [31]. Despite this, Ni<sup>2+</sup> shows superior adsorption due to its higher binding capacity and the functional groups activated during the removal process [27]. Additionally, Ni<sup>2+</sup>'s poor solubility leads to the formation of solid precipitates with the BC/PANI composite, further enhancing its removal efficiency compared to Cu<sup>2+</sup> [27]. At the same time, the hydrated ionic radius of Ni<sup>2+</sup> (0.404 nm) is smaller than Cu<sup>2+</sup> (0.419 nm) [32,33]. This strong selectivity for Ni<sup>2+</sup> contributes to its overall higher removal efficiency compared to Cu<sup>2+</sup> [34]. The ANOVA statistical analysis was performed for the Ni<sup>2+</sup> and Cu<sup>2+</sup> removal efficiencies of pure BC, pure PANI, and BC/PANI (E) with different compositions (Table 1). The p-values are  $1.72 \times 10^{-10}$  and  $1.40 \times 10^{-20}$ , respectively ( $<0.05$ ), hence there is significant difference between the performance of the adsorbents.

It is not recommended to combine excess BC with PANI via in-situ polymerization technique as this can lead to aggregation of particles when BC is used as the major constituent [35]. The addition of excess BC with PANI will negatively impacts conductivity [36]. This is due to the particle aggregation and the restriction of the movement of ions in the composite that has been prepared by in-situ polymerization [9]. This also tends to affect the mobility and diffusion of heavy metal ions to the composite [37].



**Figure 6.** (a) Ni<sup>2+</sup> and (b) Cu<sup>2+</sup> removal efficiencies of pure BC, pure PANI, and BC/PANI (E) with different weight percentages (%) of PANI.

**Table 1.** ANOVA statistical analysis of Ni<sup>2+</sup> and Cu<sup>2+</sup> removal efficiencies of pure BC, pure PANI, and BC/PANI (E) with different weight percentages (%) of PANI.

Heavy metal	Removal efficiency	SS	df	MS	F	P-value
Ni <sup>2+</sup>	Between groups	1006.6670	8	125.833	90.499	1.72 × 10 <sup>-10</sup>
	Within groups	25.0280	18	1.390		
	Total	1031.6950	26			
Cu <sup>2+</sup>	Between groups	806.7510	8	100.844	184.319	1.40 × 10 <sup>-20</sup>
	Within groups	9.8480	18	0.547		
	Total	816.5990	26			

Abbreviations: SS, Sum of squares; df, Degree of freedom; MS, Mean square

**Optimal Parameters for Ni<sup>2+</sup> Removal Efficiency**

The Ni<sup>2+</sup> removal efficiency by BC/PANI (E) (10%) by varying the weight of PANI % with 71.88% removal efficiency was chosen to optimize the removal efficiency by different parameters such as effects of adsorbent weight, contact time, and

pH. This is because the BC/PANI (50%) and (100%) indicated the removal efficiency of 75% and 79.61%, respectively, and do not demonstrate a significant increase. Given that the BC/PANI (10%) displayed a removal effectiveness of 71.88%, where the data already exhibit a good optimal removal.

*Effects of Adsorbent Weight*

Figure 7a illustrates the Ni<sup>2+</sup> removal efficiency of BC/PANI (E) using different adsorbent weights. The study evaluated weights from 0.25 to 0.75 g, revealing that the highest removal efficiency of 80.02% occurred at 0.75 g, while the lowest was 72.21% at 0.25 g. The optimal weight of 0.75 g provides sufficient reactive sites from PANI and C=O groups on BC to effectively interact with Ni<sup>2+</sup>. In contrast, lower weights limit interaction due to insufficient reactive sites [38]. Conversely, increasing the adsorbent concentration to 1 g can lead to overlapping functional sites and agglomeration, which diminishes removal efficiency of Ni<sup>2+</sup> [21].

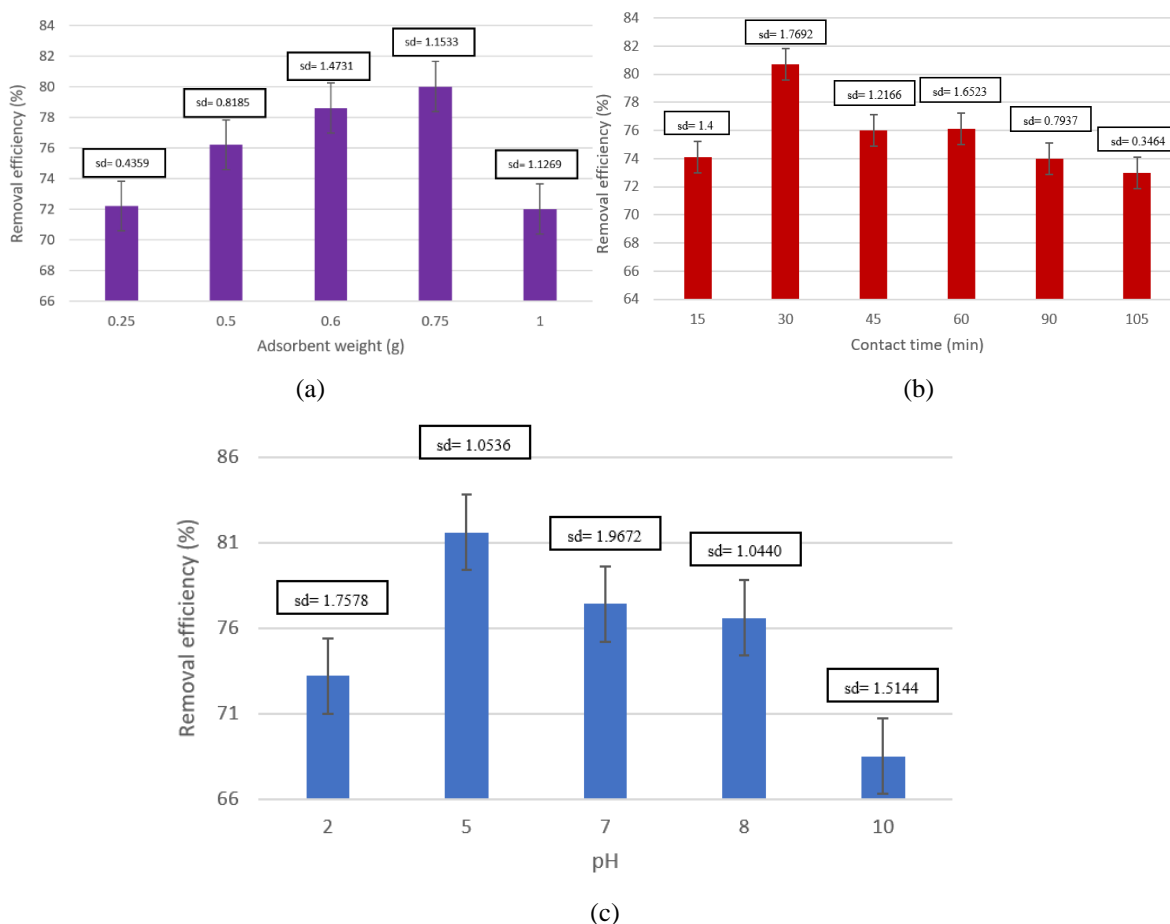
*Effects of Contact Time*

Figure 7b presents the Ni<sup>2+</sup> removal efficiency of 0.75 g of BC/PANI (E) over varying contact times from 15 to 100 minutes. The highest removal efficiency of 80.67% was achieved at 30 minutes, while the lowest was 74.1% at 15 minutes. The adsorption dynamics changes over time due to saturation and the formation of a monolayer of Ni<sup>2+</sup> ions on the adsorbent [21].

Shorter contact time results in poor removal efficiency because Ni<sup>2+</sup> lacks sufficient time to interact with the reactive sites on BC/PANI [39]. Generally, adsorption efficiency increases with longer contact time until it stabilizes at an optimal duration [40].

*Effects of pH*

Figure 7c illustrates the Ni<sup>2+</sup> removal efficiency of 0.75 g of BC/PANI (E) at different pH levels (2-10) over 30 minutes. The removal efficiency ranged from 73.32% to 81.56% in acidic conditions, with the highest efficiency observed at pH 5 (81.56%), while the lowest removal occurred at pH 10 (67.8%), an alkaline condition. In a highly acidic condition (pH 2), the binding sites of PANI will be protonated, competing with Ni<sup>2+</sup> for the available binding sites. Thus, removal efficiency may drop at pH values significantly lower than 5 [51]. At pH 5, Ni<sup>2+</sup> exists predominantly in its minimally charged form (Ni<sup>2+</sup>), which allows for optimal electrostatic interactions between the Ni<sup>2+</sup> ions and functional groups on the surface of PANI/BC. Moreover, Ni<sup>2+</sup> is rapidly precipitated into nickel(II) hydroxide (Ni(OH)<sub>2</sub>) when pH increases above 5.5, thus reducing its removal efficiency [41].



**Figure 7.** Ni<sup>2+</sup> removal efficiencies of BC/PANI (E) at different (a) adsorbent weight, (b) contact time, and (c) pH.

*Adsorption Isotherm*

The experimental data were analyzed using common equilibrium models, including Langmuir, Freundlich, Tempkin, and Dubinin-Radushkevich (D-R). Langmuir isotherm is often employed for homogeneous adsorption which occurs on monolayer forming between adsorbent and adsorbate, thus applicable mostly in gas-phase adsorption and water remediation. Although Freundlich model is comparable to Langmuir model, it is empirical and more applicable on heterogeneous surfaces or multilayer adsorption such as bio-based adsorbents and soils. On the

other hand, Tempkin model fits temperature-dependent adsorption, while D-R isotherm considers both physical and chemical adsorption processes [42, 43]. Among these, the Langmuir model provides the best fit, with the highest correlation coefficient of 0.9968, as shown in Table 2. This model suggests that Ni<sup>2+</sup> is adsorbed as a monolayer on the BC/PANI (E) adsorbent, with a maximum adsorption capacity of 4.688 mg/g. The separation factor (RL), a key parameter of the Langmuir isotherm, was calculated at 0.4996 for a 100 ppm concentration, indicating favorable adsorption conditions for Ni<sup>2+</sup> onto BC/PANI [8].

**Table 2.** Isotherm models and adsorption parameters for Ni<sup>2+</sup> removal by BC/PANI (E).

Isotherm model	Adsorption parameters
Langmuir	q <sub>m</sub> (mg/g) = 5.602 K <sub>L</sub> = 1.646 R <sub>L</sub> = 0.4996 R <sup>2</sup> = 0.9968
Freundlich	K <sub>F</sub> = 0.7661 n = 3.754 R <sup>2</sup> = 0.984
Tempkin	q <sub>e</sub> = - 1.8999 R <sup>2</sup> = 0.9584
D-R	q <sub>0</sub> = 6.177 R <sup>2</sup> = 0.8756

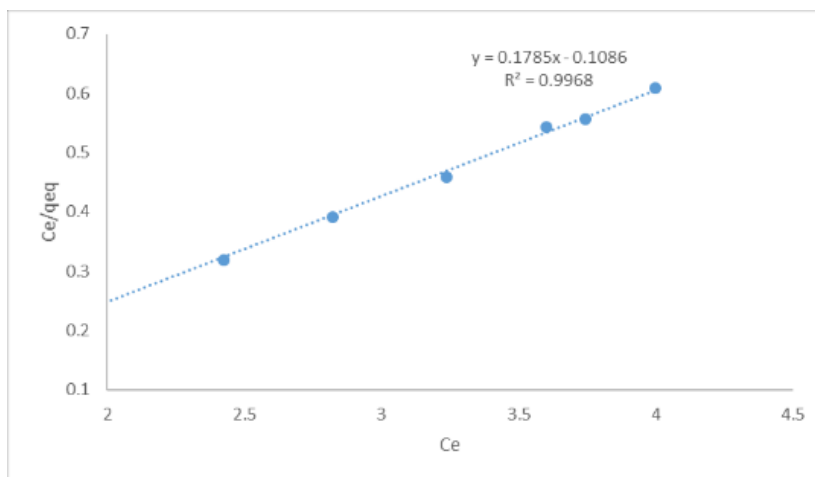


**Figure 8.** The fitted line of the Langmuir model for Ni<sup>2+</sup> removal by BC/PANI (E).

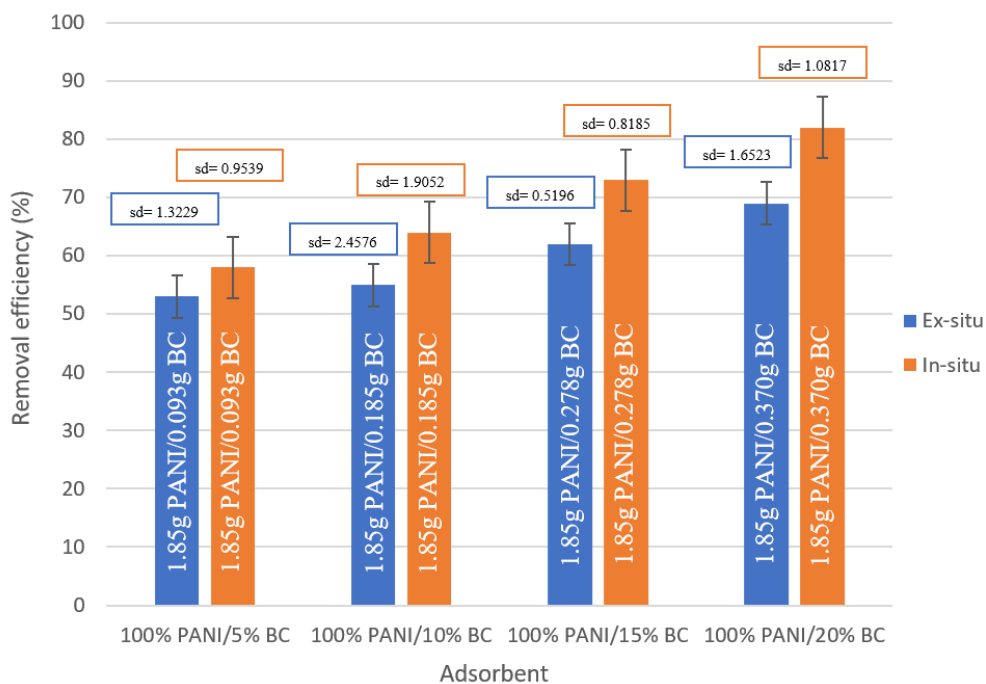


**Figure 9.** Ni<sup>2+</sup> removal efficiencies by PANI/BC (E) and PANI/BC (I) with different weights of BC%.

#### Application of BC/PANI (E) And BC/PANI (I) Composites in Ni<sup>2+</sup> Removal

Figure 9 illustrates the Ni<sup>2+</sup> removal efficiencies of PANI/BC (E) and PANI/BC (I) composites at varying BC percentages. Nickel was selected due to its superior removal efficiency, higher binding capacity, and lower precipitation tendency compared to copper [27]. For the ex-situ polymerization (PANI/BC (E)), Ni<sup>2+</sup> removal increased from 50% to 69% as BC content rose from 5% to 20%. In contrast, the in-situ polymerization (PANI/BC (I)) showed an increase from 45% to 83% under the same conditions. The highest removal efficiency achieved by PANI/BC (I) (20%) was 83%. This enhanced efficiency is linked to BC's high surface area and pore volume, which boost adsorption capacity and electrostatic interactions with Ni<sup>2+</sup> ions [44]. PANI/BC (I) outperforms PANI/BC (E) due to better interfacial bonding and uniform distribution of BC, which improves heavy metal removal [29]. The distribution of polymer chains in PANI/BC (E) might be less uniform particularly when the PANI is not chemically bonded to the surface, but instead physically adsorbed. This can lead to uneven distribution of functional groups on the BC surface, which can result in lower adsorption efficiency and selectivity. Additionally, in-situ polymerization prevents particle agglomeration and optimizes the spatial distribution within the polymer matrix, enhancing the synergistic effects of BC and PANI [45]. This can create a more evenly distributed electrostatic or chemical binding of Ni<sup>2+</sup> across the PANI/BC surface, leading to a more consistent adsorption performance.

#### CONCLUSION

In this study, pyrolyzed BC was successfully pyrolyzed and PANI was synthesized via chemical oxidation. BC/PANI composites were prepared using ex-situ polymerization, while PANI/BC composites were created through both in-situ and ex-situ methods. The chemical structure, oxidation state, surface morphology, thermal stability, and conductivity of BC, PANI, and their composites (BC/PANI (E), PANI/BC (E), and PANI/BC (I)) were confirmed through FTIR, UV-Vis, SEM, TGA, and electrical conductivity analyses. The PANI/BC (I) composite is more homogeneous and thermally stable when compared to PANI/BC (E). The BC/PANI (E) (1:1) composite achieved a removal efficiency of up to 79.61% for nickel(II) ions and 68.87% for copper(II) ions. Optimal conditions for nickel(II) removal included pH of 5, contact time of 30 minutes, and adsorbent weight of 0.75 g, resulting in 81.56% removal efficiency. Additionally, PANI/BC (E) (1:0.2) and PANI/BC (I) (1:0.2) composites removed 69% and 83% of nickel(II) ions, respectively, while using less adsorbent and requiring shorter preparation times. The Langmuir isotherm is best fitted to experimental adsorption data, indicating the adsorption occurs on homogenous monolayer surface. The superior performance of in-situ polymerized PANI/BC composites highlights their potential as efficient adsorbents for water purification, contributing to sustainable solutions for heavy metal contamination. More extensive research shall be conducted on the surface functionalization of BC and the synthesis of nano-sized PANI/BC will be considered to achieve

better interactions between the components for exceptional removal efficiency of heavy metals.

#### ACKNOWLEDGEMENT

The authors extend their appreciation to Tunku Abdul Rahman University of Management and Technology for funding the current project. Project No.:UC/I/G2023-00106, Tunku Abdul Rahman University of Management and Technology, Malaysia.

#### REFERENCES

- Gelaye, Y. (2024) Public health and economic burden of heavy metals in Ethiopia: Review. *Heliyon*, **10**(19). <https://doi.org/10.1016/j.heliyon.2024.e39022>.
- Ali, H., Khan, E., Ilahi, I. (2019) Environmental chemistry and ecotoxicology of hazardous heavy metals: Environmental persistence, toxicity, and bioaccumulation. *J. Chem.*, **2019**(Cd). <https://doi.org/10.1155/2019/6730305>.
- Qasem, N. A. A., Mohammed, R. H., Lawal, D. U. (2021) Removal of heavy metal ions from wastewater: a comprehensive and critical review. *Npj Clean Water*, **4**(1). <https://doi.org/10.1038/s41545-021-00127-0>.
- Qiu, B., Tao, X., Wang, H., Li, W., Ding, X., Chu, H. (2021) Biochar as a low-cost adsorbent for aqueous heavy metal removal: A review. *J. Anal. Appl. Pyrolysis*, **155**, 105081, December 2020. <https://doi.org/10.1016/j.jaap.2021.105081>.
- Saharudin, D. M., Jeswani, H. K., Azapagic, A. (2024) Biochar from agricultural wastes: Environmental sustainability, economic viability and the potential as a negative emissions technology in Malaysia. *Sci. Total Environ.*, **919**, 170266 (January). <https://doi.org/10.1016/j.scitotenv.2024.170266>.
- Sintim, H. Y., Flury, M. (2017) Is Biodegradable Plastic Mulch the Solution to Agriculture's Plastic Problem? *Environ. Sci. Technol.*, **51**(3), 1068–1069. <https://doi.org/10.1021/acs.est.6b06042>.
- Kukulski, T., Stainstaw Waclawek, Daniele, K. K., Padil, V. V. T., Fryczkowski, R., Jarosław Janicki, M. C., (2020) Polymers A Polymeric Composite Material (rGO / PANI) for Acid Blue 129 Adsorption. *Polymers (Basel)*, **12**(1051), 1–13.
- Senguttuvan, S., Senthilkumar, P., Janaki, V., Kamala-Kannan, S. (2021) Significance of conducting polyaniline based composites for the removal of dyes and heavy metals from aqueous solution and wastewaters - A review. *Chemosphere*, **267**, 129201. <https://doi.org/10.1016/j.chemosphere.2020.129201>.
- Thomas, D., Fernandez, N. B., Mullassery, M. D., Surya, R., Jacob, L. E. (2023) Banana stem biochar composite with polyaniline for energy storage applications. *Results Chem.*, **6**, 101088 (August). <https://doi.org/10.1016/j.rechem.2023.101088>.
- El-Shazly, A. H., Elkady, M., Abdelraheem, A. (2022) Investigating the Adsorption Behavior of Polyaniline and Its Clay Nanocomposite towards Ammonia Gas. *Polymers (Basel)*, **14**(21). <https://doi.org/10.3390/polym14214533>.
- Wang, Q., Huang, M., Zhu, Y., Wang, J., He, Z., Liu, J., Sun, K., Li, Z., Deng, G. (2023) Polyaniline-modified halloysite nanotubes as high-efficiency adsorbents for removing of naproxen in the presence of different heavy metals. *RSC Adv.*, **13**(34), 23505–23513. <https://doi.org/10.1039/d3ra03671e>
- Rahim, S. A., Bong, C. K. W., Mohd Danial, N. F., Salim, A., Supardi, N. R., Zahari, N. Z., Cleophas, F., Tair, R., Musta, B. (2024) Heavy Metal Pollution in Water and Sediment of Lohan River, Ranau, Sabah, Malaysia. *J. Environ. Microbiol. Toxicol.*, **12**(2), 44–52.
- Ruzi, I. I., Ishak, A. R., Abdullah, M. A., Zain, N. N. M., Tualeka, A. R., Adriyani, R., Mohamed, R., Edinur, H. A., Aziz, M. Y. (2024) Heavy metal contamination in Sungai Petani, Malaysia: a wastewater-based epidemiology study. *J. Water Health*, **22**(6), 953–966. <https://doi.org/10.2166/wh.2024.241>.
- Elnour, A. Y., Alghyamah, A. A., Shaikh, H. M., Poulouse, A. M., Al-Zahrani, S. M., Anis, A., Al-Wabel, M. I. (2019) Effect of pyrolysis temperature on biochar microstructural evolution, physicochemical characteristics, and its influence on biochar/polypropylene composites. *Appl. Sci.*, **9**(6), 7–9. <https://doi.org/10.3390/app9061149>.
- Parveen, A., Manjunatha, S., Kumar, M. M., Roy, A. S. (2024) Agile soft template array fabrication of one-dimensional (1D) polyaniline nanocomposite fibers for hydrogen storage. *RSC Adv.*, **14**(35), 25347–25358. <https://doi.org/10.1039/d4ra04710a>.
- Idrees, R., Shah, S. A. A., Omer, S., Mehmood, Z., Saeed, S. (2024) Preparation and investigation of Montmorillonite-K10 Polyaniline nanocomposites for optoelectronic applications. *Heliyon*, **10**(6), e27573. <https://doi.org/10.1016/j.heliyon.2024.e27573>.
- Eltaweil, A. S., Abdelfatah, A. M., Hosny, M., Fawzy, M. (2022) Novel Biogenic Synthesis of a Ag@Biochar Nanocomposite as an Antimicrobial Agent and Photocatalyst for Methylene Blue Degradation. *ACS Omega*, **7**(9), 8046–8059. <https://doi.org/10.1021/acsomega.1c07209>.

- 172 Ravi Varma Sudaya, Min Rui Chia, Peratiikka Selvam, Sook-Wai Phang and Kian Wei Chong
- Enhanced Removal of Ni<sup>2+</sup> and Cu<sup>2+</sup> Using Biochar/Polyaniline Composites: A Comparative Study of In-Situ and Ex-Situ Polymerization Methods
18. Babaei, Z., Rezaei, B., Gholami, E., Afshar Taromi, F., Haghighi, A. H. (2024) In situ synthesis of long tubular water-dispersible polyaniline with core/shell gold and silver@graphene oxide nano-particles for gas sensor application. *Heliyon*, **10(4)**, e26662. <https://doi.org/10.1016/j.heliyon.2024.e26662>.
  19. Kumar, B., Adil, S., Pham, D. H., Kim, J. (2024) Environment-friendly, high-performance cellulose nanofiber-vanillin epoxy nanocomposite with excellent mechanical, thermal insulation and UV shielding properties. *Heliyon*, **10(3)**, e25272. <https://doi.org/10.1016/j.heliyon.2024.e25272>.
  20. Thomas, D., Fernandez, N. B., Mullassery, M. D., Surya, R. (2020) Iron oxide loaded biochar/polyaniline nanocomposite: Synthesis, characterization and electrochemical analysis. *Inorg. Chem. Commun.*, **119**, 108097 (May). <https://doi.org/10.1016/j.inoche.2020.108097>.
  21. Yakişik, H., Özveren, U. (2021) Synthesis of polyaniline/biochar composite material and modeling with nonlinear model for removal of copper (II) heavy metal ions. *J. Turkish Chem. Soc. Sect. A Chem.*, **8(1)**, 291–304. <https://doi.org/10.18596/jotcsa.635073>.
  22. Fouda-Mbanga, B. G., Onotu, O. P., Tywabi-Ngeva, Z. (2024) Advantages of the reuse of spent adsorbents and potential applications in environmental remediation: A review. *Green Anal. Chem.*, **11**, 100156 (August). <https://doi.org/10.1016/j.greac.2024.100156>.
  23. Zaitun, Z., Halim, A., Sa'dah, Y., Cahyadi, R. (2022) Surface morphology properties of biochar feedstock for soil amendment. *IOP Conf. Ser. Earth Environ. Sci.*, **951(1)**. <https://doi.org/10.1088/1755-1315/951/1/012034>.
  24. Chao, D., Chen, J., Lu, X., Chen, L., Zhang, W., Wei, Y. (2005) SEM study of the morphology of high molecular weight polyaniline. *Synth. Met.*, **150(1)**, 47–51. <https://doi.org/10.1016/j.synthmet.2005.01.010>.
  25. Herath, A., Reid, C., Perez, F., Pittman, C. U., Mlsna, T. E. (2021) Biochar-supported polyaniline hybrid for aqueous chromium and nitrate adsorption. *J. Environ. Manage.*, **2961**, 30. <https://doi.org/10.1016/j.jenvman.2021.113186>.
  26. Jose, A., Yadav, P., Svirskis, D., Swift, S., Gizdavic-Nikolaidis, M. R. (2024) Antimicrobial photocatalytic PANI based-composites for biomedical applications. *Synth. Met.*, **303**, 117562 (January). <https://doi.org/10.1016/j.synthmet.2024.117562>.
  27. Doyo, A. N., Kumar, R., Barakat, M. A. (2023) Facile Synthesis of the Polyaniline@Waste Cellulosic Nanocomposite for the Efficient Decontamination of Copper(II) and Phenol from Wastewater. *Nanomaterials*, **13(6)**. <https://doi.org/10.3390/nano13061014>.
  28. Li, R., Liu, L., Yang, F. (2014) Removal of aqueous Hg(II) and Cr(VI) using phytic acid doped polyaniline/cellulose acetate composite membrane. *J. Hazard. Mater.*, **280**, 20–30. <https://doi.org/10.1016/j.jhazmat.2014.07.052>.
  29. Mohammad, S. G., Abulyazied, D. E., Ahmed, S. M. (2019) Application of polyaniline/activated carbon nanocomposites derived from different agriculture wastes for the removal of Pb(II) from aqueous media. *Desalin. Water Treat.*, **170**, 199–210. <https://doi.org/10.5004/dwt.2019.24694>.
  30. Azzam, E. M. S., Elsofany, W. I., Alrashdi, G. K., Alenezi, K. M., Alsukaibi, A. K. D., Latif, S., Abdulaziz, F., Atta, A. M. (2022) New route for removal of Cu(II) using fabricated nanocomposite based on cationic surfactant/Ag-nanoparticles/silica gel. *Arab. J. Chem.*, **15(7)**, 103897. <https://doi.org/10.1016/j.arabjc.2022.103897>.
  31. Wang, J., Deng, B., Chen, H., Wang, X., Zheng, J. (2009) Removal of Aqueous Hg(II) by Polyaniline: Sorption Characteristics and Mechanisms. *J. Environ. Sci. Technol.*, **43(14)**, 5223–5228.
  32. Atif, M., Ul Husnain, H., Ur Rehman, A., Younas, U., Rafique, T., Khalid, W., Ali, Z., Nadeem, M., (2024) Enhancement in the dielectric and magnetic properties of Ni<sup>2+</sup>–Cu<sup>2+</sup> co-doped BaFe<sub>11</sub>Cu<sub>1–x</sub>Ni<sub>x</sub>O<sub>19</sub> hexaferrites (0.0 ≤ x ≤ 1.0). *RSC Adv.*, **14(10)**, 6883–6895. <https://doi.org/10.1039/d3ra06684c>.
  33. Chen, P. W., Hsiao, M. N., Xiao, L. W., Liu, Z. S. (2024) Adsorption behavior of heavy metals onto microplastics derived from conventional and biodegradable commercial plastic products. *Sci. Total Environ.*, **951**, 175537 (May). <https://doi.org/10.1016/j.scitotenv.2024.175537>.
  34. Marciniak, M., Goscińska, J., Frankowski, M., Pietrzak, R. (2019) Optimal synthesis of oxidized mesoporous carbons for the adsorption of heavy metal ions. *J. Mol. Liq.*, **276**, 630–637. <https://doi.org/10.1016/j.molliq.2018.12.042>.
  35. Hajjaoui, H., Soufi, A., Boumya, W., Abdennouri, M., Barka, N. (2021) Polyaniline/nanomaterial composites for the removal of heavy metals by adsorption: A review. *J. Compos. Sci.*, **5(9)**. <https://doi.org/10.3390/JCS5090233>.

36. Liu, P., Guo, X., Nan, F., Duan, Y., Zhang, J. (2016) Modifying mechanical, optical properties and thermal Processability of iridescent cellulose nanocrystal films using ionic liquid. *ACS Appl. Mater. Interfaces*, **9**(3), 3085–3092. <https://doi.org/10.1021/acsami.6b12953>.
37. El Mahdaoui, A., Radi, S., Elidrissi, A., Faustino, M. A. F., Neves, M. G. P. M. S., Moura, N. M. M. (2024) Progress in the modification of cellulose-based adsorbents for the removal of toxic heavy metal ions. *J. Environ. Chem. Eng.*, **12**(5), 113870. <https://doi.org/10.1016/j.jece.2024.113870>.
38. Birniwa, A. H., Kehili, S., Ali, M., Musa, H., Ali, U., Kutty, S. R. M., Jagaba, A. H., Abdullahi, S. S., Tag-Eldin, E. M., Mahmud, H. N. M. E. (2022) Polymer-Based Nano-Adsorbent for the Removal of Lead Ions: Kinetics Studies and Optimization by Response Surface Methodology. *Separations*, **9**(11). <https://doi.org/10.3390/separations9110356>.
39. Khong, C. H., Teh, G. B., Phang, S. W. (2018) Effect of Titanium Dioxide and Carbon Nanotubes on Polyaniline Nanocomposites for Heavy Metals Removal. *Macromol. Symp.*, **382**(1), 1–8. <https://doi.org/10.1002/masy.201800087>.
40. Manimekalai, B., Subramanian, S. (2024) Synthesized bioadsorbent using Aged Refuse for heavy metal removal in aqueous solution. *Desalin. Water Treat.*, **320**(100862), 1–25. <https://doi.org/10.1016/j.dwt.2024.100862>.
41. Tawonezvi, T., Zide, D., Nomnqa, M., Madondo, M., Petrik, L., Bladergroen, B. J. (2024) Recovery of NMC(OH)<sub>2</sub> and Li<sub>2</sub>CO<sub>3</sub> from spent Li-ionB cathode leachates using non-Na precipitant-based chemical precipitation for sustainable recycling. *Chem. Eng. J. Adv.*, **17**, 100582 (December 2023). <https://doi.org/10.1016/j.cej.2023.100582>.
42. Faruque, M. O., Uddin, S., Hossain, M. M., Hossain, S. M. Z., Shafiquzzaman, M., Razzak, S. A. (2024) A comprehensive review on microalgae-driven heavy metals removal from industrial wastewater using living and nonliving microalgae. *J. Hazard. Mater. Adv.*, **16**, 100492 (August). <https://doi.org/10.1016/j.hazadv.2024.100492>.
43. Sharma, G., Verma, Y., Lai, C. W., Naushad, M., Iqbal, J., Kumar, A., Dhiman, P. (2024) Biochar and biosorbents derived from biomass for arsenic remediation. *Heliyon*, **10**(17), e36288. <https://doi.org/10.1016/j.heliyon.2024.e36288>.
44. Amarasekara, A. S., Shrestha, A. B., Wang, D. (2024) Chemical modifications of kombucha SCOBY bacterial cellulose films by citrate and carbamate cross-linking. *Carbohydr. Polym. Technol. Appl.*, **8**, 100595 (November). <https://doi.org/10.1016/j.carpta.2024.100595>.
45. Guo, Q., Ghadiri, R., Weigel, T., Aumann, A., Gurevich, E. L., Esen, C., Medenbach, O., Cheng, W., Chichkov, B., Ostendorf, A. (2014) Comparison of in situ and ex situ methods for synthesis of two-photon polymerization polymer nanocomposites. *Polymers (Basel)*, **6**(7), 2037–2050. <https://doi.org/10.3390/polym6072037>.